FEEDBACK CONTROL LAWS FOR HIGHLY MANEUVERABLE AIRCRAFT

NASA GRANT NAG 1 - 1380

ANNUAL REPORT
FEBRUARY 1, 1995 TO JANUARY 31, 1996

SUBMITTED TO

NASA LANGLEY RESEARCH CENTER

January 31, 1995

BY

WILLIAM L. GARRARD AND GARY J. BALAS
DEPARTMENT OF AEROSPACE ENGINEERING AND MECHANICS
UNIVERSITY OF MINNESOTA
MINNEAPOLIS, MN 55455

FEEDBACK CONTROL LAWS FOR HIGHLY MANEUVERABLE AIRCRAFT

Annual Report for the Period February 1, 1994 to January 31, 1995

During this year, we concentrated our efforts on the design of controllers for lateral/directional control using μ synthesis. This proved to be a more difficult task than we anticipated and we are still working on the designs.

In the lateral-directional control problem, the inputs are pilot lateral stick and pedal commands and the outputs are roll rate about the velocity vector and side slip angle. The control effectors are ailerons, rudder deflection, and directional thrust vectoring vane deflection which produces a yawing moment about the body axis. Our math model does not contain any provision for thrust vectoring of rolling moment. This has resulted in limitations of performance at high angles of attack.

During 1994-95, accomplished the following tasks for the lateral-directional controllers:

1. Designed both inner and outer loop dynamic inversion controllers. These controllers are implemented using accelerometer outputs rather than an a priori model of the vehicle aerodynamics.

2. Used classical techniques to design controllers for the system linearized by dynamics inversion. These controllers acted to control roll rate and Dutch roll response.

3. Implemented the inner loop dynamic inversion and classical controllers on the 6 DOF simulation.

4. Developed a lateral - directional control allocation scheme based on minimizing required control effort among the ailerons, rudder, and directional thrust vectoring.

5. Developed μ outer loop controllers combined with classical inner loop controllers.

Dynamic inversion is used to cancel the aerodynamic and inertial cross coupling torque about the pitch, roll and yaw axes. Pseudo controls are used to generate commands to the actual control effectors which are ailerons, rudder and directional thrust vector vane deflection. The inputs to the inner loop controller are the roll and yaw rate commands and the outputs are the roll and yaw rates so that a 2x2 transfer matrix relates the inputs and outputs. Ideally this matrix would be diagonal with the non - zero terms integrators. The effects of uncertainties in the aerodynamics will result in incomplete cancellation of the system dynamics by the dynamic inversion control laws.

The design of the lateral - directional controllers was considerably more complex than that of the longitudinal controllers. One complication was introduced by the fact that the lateral handling qualities vary substantially more with angle of attack than do longitudinal handling qualities. In the case of the longitudinal controller design it was possible to find a single short period natural frequency and damping factor which satisfied the handling quality specifications for all flight conditions. This was not the case for the lateral handling qualities. At higher angles of attack a much longer time constant (lower bandwidth) is required for level one handling qualities. This resulted in the necessity for designing different μ controllers for different angles of attack. These controllers then had to be scheduled with flight condition. Since these controllers differed considerably from one another in terms of pole-zero configurations, simple gain scheduling was not useful in controller scheduling. After considerable effort, we were unable to develop a realistic method for controller scheduling; therefore, we developed another approach.

The complexity and the large differences between the directional controllers at various flight conditions was the main obstacle in the scheduling. In order to simplify the controllers, first-order inner loop classical yaw and roll rate controllers were designed. The bandwidths of these controllers were scheduled with flight conditions to meet handling quality specifications. Then μ controllers were designed for outer loop side slip control. The frequency response of these μ side slip controllers were similar at various angles of attack and we were able to select a baseline μ controller to be used at all angles of attack. The inputs to this controller were filtered in such a way that at other flight conditions, the overall input/output relationships were very close to the

μ controllers. These filters were simple pole and zero cascades scheduled with flight conditions.

The design of the lateral-directional control laws has taken more time than we anticipated; therefore, we have requested an additional years extension at no cost extension. Our work during the fourth year will include the following topics:

1 Completion of the design of outer loop control laws using μ synthesis.

2. Evaluation of stability and performance robustness of control laws
   using real and complex uncertainty models.

3. Integration of the longitudinal dynamic inversion controllers designed previously with the lateral-directional control laws currently under design

4. Evaluation of performance of the integrated lateral-directional and longitudinal μ/dynamic inversion controllers using nonlinear computer simulations.

In previous studies we did not use the full complement of sensors available. In this study we will use all sensors and we will incorporate weightings on the sensors so that the control laws will optimize the use of the sensors based on their accuracy and frequency response characteristics.

Robustness will be determined by structured singular value analyses in which errors are modeled as real or complex depending on their physical nature. Variations in aerodynamic coefficients, for example, will be represented by real perturbations in the coefficients of the equations of motion. Other errors, such as high frequency dynamics and sensor errors, will be represented as complex functions as they are dynamic in nature and can be modeled as transfer functions

We have shown in our previous work that linear analyses can be very useful but are not adequate to determine important quantities such as peak acceleration and side slip during extreme maneuvers. Thus we

will test our control laws using nonlinear simulations. Maneuvers such as velocity vector rolls and turns at high angles of attack will be emphasized.

Publications Resulting From the Grant

Jacob Reiner, Gary J. Balas, and William L. Garrard, "Design of a Flight Control System for a Highly Maneuverable Aircraft Using Robust Dynamic Inversion," *Journal of Guidance Control and Dynamics*, An - Feb. 1995.

Jacob Reiner, Gary J. Balas, and William L. Garrard, "Design of Flight Control System Using Robust Dynamic Inversion with Time Scale Separation," accepted *Automatica*, 1995.

Gary J. Balas, William L. Garrard, and Jacob Reiner, "Robust Dynamic Inversion Control Laws for Aircraft Control," AIAA Paper No. 92 - 4329 AIAA Guidance, Navigation and Control Conference, Hilton Head, South Carolina, August 1992.

Gary J. Balas, Jacob Reiner, William L. Garrard, "Design of a Flight Control System for a Highly Maneuverable Aircraft Using μ Synthesis," AIAA Guidance Navigation and Control Conference, August 1993, Monterey, California.

Gary J. Balas, Jacob Reiner, William L. Garrard, "Design of a Flight Control System for a Highly Maneuverable Aircraft Using Robust Dynamic Inversion," AIAA Guidance Navigation and Control Conference, August 1994, Phoenix, Arizona.

Sadok Hougui, Gary J. Balas, William L. Garrard, "Design of a Robust Dynamic Inversion Lateral/Directional Flight Controller," submitted to AIAA Guidance Navigation and Control Conference, August 1995, Baltimore, Maryland.

Degrees Awarded as a Result of the Grant

Jacob Reiner, Ph.D. in Aerospace Engineering University of Minnesota *Control Design for Aircraft Using Robust Dynamic Inversion Technique*, July 1993.

JOURNAL OF GUIDANCE, CONTROL, AND DYNAMICS
Vol. 32, No. 2, March–April 1995

Robust Dynamic Inversion for Control of Highly Maneuverable Aircraft

Jacob Reiner,* Gary J. Balas,† and William L. Garrard‡
University of Minnesota, Minneapolis, Minnesota 55455

This paper presents a methodology for the design of flight controllers for aircraft operating over large ranges of angle of attack. The methodology is a combination of dynamic inversion and structured singular value (μ) synthesis. An inner-loop controller, designed by dynamic inversion, is used to linearize the aircraft dynamics. This inner-loop controller lacks guaranteed robustness to uncertainties in the system model and the measurements; therefore, a robust, linear outer-loop controller is designed using μ synthesis. This controller minimizes the weighted H_∞ norm of the error between the aircraft response and the specified handling quality model while maximizing robustness to model uncertainties and sensor noise. The methodology is applied to the design of a pitch rate command system for longitudinal control of a high-performance aircraft. Nonlinear simulations demonstrate that the controller satisfies handling quality requirements, provides good tracking of pilot inputs, and exhibits excellent robustness over a wide range of angles of attack and Mach number. The linear controller requires no scheduling with flight conditions.

I. Introduction

THE objective of this paper is to present a method for design of flight controllers that provides desired handling qualities over a wide range of flight conditions with minimal scheduling. Acceptable stability and performance robustness must be maintained in the presence of unmodeled dynamics, uncertainties in the aircraft design model, and noisy sensor measurements.

The aircraft considered in this paper is the NASA high angle-of-attack research vehicle (HARV), which is typical of future fighter aircraft. It is capable of flight at very high angles of attack and has thrust vectoring as well as conventional aerodynamic control surfaces.[1] The unaugmented aircraft does not meet handling quality requirements and some type of augmentation is necessary. This paper considers only the longitudinal control. The controller relates pilot longitudinal stick input to the symmetric deflection of the stabilizer and the longitudinal deflection of the thrust vectoring vanes.

The control design philosophy is to use an inner-loop, dynamic inversion controller and an outer-loop, linear μ controller. The dynamic inversion controller linearizes the pitch rate dynamics of the aircraft; however, since model uncertainties prevent exact linearization, there will always be errors associated with this controller. A simple linear fractional transformation model of these errors is developed for use in design of the outer-loop μ controller. This controller provides pitch rate following by minimizing the weighted H_∞-norm of the difference between the actual aircraft pitch rate response to pilot stick inputs and the desired response to these inputs as given by a transfer function model based on standard handling quality specifications. Thus the outer-loop μ controller is an implicit model following design, which provides robustness to errors due to the lack of exact cancellation of the pitch rate dynamics by the dynamic inversion controller.

Recently a number of papers have appeared that describe controllers for a highly maneuverable aircraft. In Refs. 2–5, application of linear multi-input/multi-output (MIMO) control design techniques to this problem were presented. In every case, excellent local performance was achieved, although robustness outside the linear region was not guaranteed. For a global design, gain scheduling is required. Gain scheduling of MIMO controllers can be complicated, and an alternative is to use control design methods that directly consider the nonlinear nature of the problem. One such alternative is dynamic inversion.

The control of nonlinear systems through the use of their inverse dynamics is a topic that has received a great deal of attention in recent years.[6–13] Lane and Stengel[13] recommended implementing such controllers to improve levels of performance and safety over conventional flight controller designs. The idea of applying dynamic inversion to highly maneuverable aircraft operating in the post-stall regime was presented in Refs. 14–16. The simulations and tests described in the first two references and the Lyapunov analysis in the third show that dynamic inversion is a good candidate for control of aircraft operating at high angles of attack and/or at high angular rates. The main assumptions in Refs. 14–16 are 1) the governing equations are known precisely and 2) the aircraft states are measured or estimated accurately. If either of these requirements are not met, the cancellation of the nonlinear dynamics will not be exact. This may have serious consequences since dynamic inversion by itself does not guarantee any robustness to modeling uncertainties. Moreover, even though the nominal inverted system is designed to follow handling quality requirements, it can be shown that when the inversion of the aircraft dynamics is not perfect, the closed-loop aircraft response may not meet those requirements.[17] Stability and performance robustness within the dynamic inversion framework are addressed by synthesizing a robust, outer-loop controller around the dynamic inversion inner loop. The outer-loop controller is designed using structured singular value (μ) techniques.

The proposed technique results in the dynamics from the desired input to the controlled output being linear and constant over the entire flight regime. Therefore, gain scheduling complexity is substantially decreased or even avoided through the use of dynamic inversion. The input/output relations are not identical over the flight regime since the feedback linearization achieved using dynamic inversion is not perfect. However, a single μ controller can be synthesized in conjunction with a linearizing feedback such that the closed-loop system is robustly stable and meets a predefined desired handling quality specification over a significant portion of the flight envelope.

II. Dynamic Inversion

Dynamic inversion is a technique in which feedback is used to linearize the system to be controlled and to provide desired dynamic response.[18,19] In this paper, dynamic inversion is used to linearize

Received May 24, 1993; revision received June 2, 1994; accepted for publication June 28, 1994.

*[job title], Department of Aerospace Engineering and Mechanics; currently Senior Guidance and Control Engineering, Rafael, Haifa, Israel. Member AIAA.

†Assistant Professor, Department of Aerospace Engineering and Mechanics. Member AIAA.

‡Professor, Department of Aerospace Engineering and Mechanics. Fellow AIAA.

the pitch rate dynamics of the aircraft. The equation of motion for the pitching dynamics is

$$\dot{q} = \frac{I_{xz}}{I_{yy}}(r^2 - p^2) - \frac{(I_{zz} - I_{xx})rp}{I_{yy}} + \frac{M_a}{I_{yy}} + \frac{M_c}{I_{yy}} \tag{1}$$

where p, q, and r are the roll, pitch, and yaw rates, respectively, in body axes coordinates; M_a is the aerodynamic pitching moment excluding the moment from the aerodynamic control surfaces; and M_c is the control moment due to aerodynamic surfaces and thrust vectoring. Dynamic inversion uses the control moment to cancel the dynamics of the aircraft and insert a desired response $\dot{q}_d$. Ideally, this results in a linear input/output relationship from the desired input $\dot{q}_d$ to the actual output $\dot{q}$. Denoting the measured angular rates and estimated aerodynamic and physical data by hats ($\hat{}$), the commanded moment is

$$M_c = -\left[\frac{\hat{I}_{xz}}{\hat{I}_{yy}}(\hat{r}^2 - \hat{p}^2) - \frac{(\hat{I}_{zz} - \hat{I}_{xx})\hat{r}\hat{p}}{\hat{I}_{yy}} + \frac{\hat{M}_a}{\hat{I}_{yy}}\right] + \dot{q}_d \tag{2}$$

If all of the data and measurements are available with no errors, the control law defined in Eq. (2) results in $\dot{q} = \dot{q}_d$.

In the HARV, the commanded moment is implemented by deflection commands to the aerodynamic surfaces δ_s and the trust vectoring vanes δ_{tvc}. The allocation of effort between these two surfaces can be accomplished by a variety of methods and is the subject of recent research.[14-16] The usual procedure is to use aerodynamic control for small maneuvers with thrust vectoring being incorporated where needed. In this paper, a simple minimum control energy algorithm for allocating effort was used; however, the dynamic inversion design procedure will work equally well with other control allocation schemes.[14-16] In this paper, the deflections are allocated to minimize the cost function

$$J = \frac{1}{2}\left[\left(\frac{\delta_s}{|\delta_s|_{\max}}\right)^2 + \left(\frac{\delta_{tvc}}{|\delta_{tvc}|_{\max}}\right)^2\right] \tag{3}$$

subject to the constraint

$$M_c = \hat{M}_{\delta_{tvc}}\delta_{tvc} + \hat{M}_{\delta_s}\delta_s \tag{4}$$

where $\hat{M}_{\delta_{tvc}}$ and $\hat{M}_{\delta_s}$ are the estimated values of the thrust vector and stabilizer moment derivatives. Minimization of J results in the commanded deflections given next:

$$\delta_{tvc_c} = \frac{M_c/\hat{M}_{\delta_{tvc}}}{1 + \left(\hat{M}^2_{\delta_s}|\delta_s|^2_{\max}\right)/\left(\hat{M}^2_{\delta_{tvc}}|\delta_{tvc}|^2_{\max}\right)} = \hat{K}_{tvc}M_c \tag{5}$$

$$\delta_{s_c} = \frac{M_c/\hat{M}_{\delta_s}}{1 + \left(\hat{M}^2_{\delta_{tvc}}|\delta_{tvc}|^2_{\max}\right)/\left(\hat{M}^2_{\delta_s}|\delta_s|^2_{\max}\right)} = \hat{K}_s M_c \tag{6}$$

The stabilizer becomes ineffective at higher angles of attack. This results in a small value of $\hat{M}_{\delta_s}$, and most of the control torque is supplied by thrust vectoring. At lower angles of attack, thrust vectoring and the stabilizer play more equal roles. The commanded deflections are the same as the actual deflections when the actuatordynamics are neglected, so that the actual control moment is

$$M_c = \left(M_{\delta_s}\hat{K}_s + M_{\delta_{tvc}}\hat{K}_{tvc}\right) \times \left[-\frac{\hat{I}_{xz}}{\hat{I}_{yy}}(\hat{r}^2 - \hat{p}^2) + \frac{\hat{I}_{zz} - \hat{I}_{xx}}{\hat{I}_{yy}}\hat{r}\hat{p} - \hat{M}_a + \dot{q}_d\right] \tag{7}$$

The term M_a is approximated in the dynamic inversion implementation using a least-squares representation of the aerodynamic data

$$M_a \approx \tfrac{1}{2}\rho V^2 S_{ref} C_{ref}\left[C_{m_a}(\alpha) + \frac{C_{ref}}{2V}C_{m_q}(\alpha)q\right] \equiv m_a + m_q q \tag{8}$$

Inserting Eqs. (7) and (8) into Eq. (1) leads to the following pitch acceleration equation:

$$\dot{q} = \frac{I_{xz}}{I_{yy}}(r^2 - p^2) - \frac{I_{zz} - I_{xx}}{I_{yy}}rp + m_a + m_q q + \left(M_{\delta_s}\hat{K}_s + M_{\delta_{tvc}}\hat{K}_{tvc}\right) \times \left[-\frac{\hat{I}_{xz}}{\hat{I}_{yy}}(\hat{r}^2 - \hat{p}^2) + \frac{\hat{I}_{zz} - \hat{I}_{xx}}{\hat{I}_{yy}}\hat{r}\hat{p} - \hat{m}_a - \hat{m}_q\hat{q} + \dot{q}_d\right] \tag{9}$$

Equation (9) is the actual closed-loop input/output relation after applying feedback linearization. From Eqs. (5) and (6), it can be observed that if $K_{tvc} = \hat{K}_{tvc}$ and $K_s = \hat{K}_s$, then $M_{\delta_s}\hat{K}_s + M_{\delta_{tvc}}\hat{K}_{tvc} = 1$. Moreover, if all of the estimated data and measurements are exact, then Eq. (9) yields an exact linear relation $\dot{q} = \dot{q}_d$.

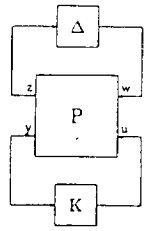

Fig. 1 General interconnection structure.

III. μ Synthesis

Feedback linearization described assumes exact knowledge of the system. Practically this is not the case. To address robustness to measurements and model uncertainties, an outer-loop controller is designed based on structured singular value (μ) techniques.[19-23]

The general framework of μ synthesis, shown in Fig. 1, is based on describing the system as a linear fractional transformation (LFT). Any linear interconnection of inputs, outputs, and commands along with perturbations and a controller can be viewed in this context and rearranged to match this diagram. The term P represents the system interconnection structure, Δ the uncertainties, and K the control law. The vector y is composed of measurement signals provided to the controller, u is a vector of inputs from the control law, and z and w are the inputs and outputs of the uncertainty block. Robust performance of the closed-loop system is achieved if all of the performance requirements, given in terms of the weighted H_∞ norm, are satisfied for all possible plants as defined by the uncertainty description Δ. The Δ block is normalized to 1 for the synthesis procedure.

The synthesis problem involves finding a stabilizing controller K such that the performance requirements are satisfied under prescribed uncertainties. The D–K iteration, which is an approximation to μ synthesis, is a practical approach to design control systems with the goal of robust performance.[23-25] This technique integrates H_∞ optimization methods for controller synthesis and the structured singular value for analysis. An upper bound of μ is found by scaling the closed-loop system with a scaling matrix D obtained from solving the μ analysis problem. The problem of robust controller design becomes that of finding a stabilizing controller K and a scaling matrix D such that the quantity $\|DF_l(P, K)D^{-1}\|_\infty$ is minimized. One approach to solving this problem is to alternatively minimize the preceding expression for either K or D while holding the other constant. For a fixed D, an H_∞ optimal control problem is solved using the well-known state-space method.[21,26] On the other hand, with fixed K, the preceding quantity can be minimized at each frequency as a convex optimization in $\ln(D)$.[21,23,25] The resulting data of D can be fit with an invertible, stable, minimum-phase, real-rational transfer function. This D–K iteration process is carried out until a satisfactory controller is constructed.

IV. Error Modeling

We now need to develop a model of the errors implicit in Eq. (9) to construct our robust outer-loop controller. For purposes of

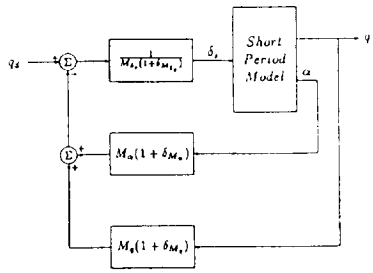

Fig. 2 Linear formulation for dynamic inversion analysis.

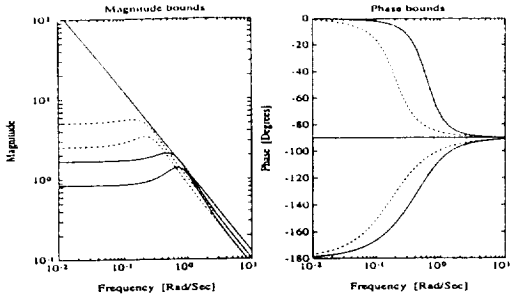

Fig. 3 Magnitude and phase bounds of possible $q/\dot{q}_d$ transfer functions at $\alpha = 5$ (full) and 35 deg (dashed).

formulating this error model we assume that $\dot{r} = \dot{p} = r = p = 0$. The model is further simplified by modeling the input as a single uncertain effector. Incorporating these assumptions into Eq. (9) and linearizing results in the following simplified closed-loop pitch rate dynamics,

$$\begin{bmatrix} \dot{\alpha} \\ \dot{q} \end{bmatrix} = \begin{bmatrix} Z_\alpha & (1+Z_q) \\ M_\alpha & M_q \end{bmatrix} \begin{bmatrix} a \\ q \end{bmatrix} + \begin{bmatrix} Z_{\delta_s} \\ M_{\delta_s} \end{bmatrix} \left[\frac{1}{\hat{M}_{\delta_s}} (\dot{q}_d - \hat{M}_\alpha \alpha - \hat{M}_q q) \right] \tag{10}$$

The set of all possible transfer functions from $\dot{q}$ to $\dot{q}_d$ is defined by varying the stability derivatives M_q, M_α, and M_{δ_s} from their nominal values. The uncertainty descriptions can include model errors in the measurements as well as uncertainties in the aerodynamic coefficients. Since the level of uncertainty in the aerodynamic parameters was not given, a maximum uncertainty of 20% is estimated for each of the stability derivatives. A linear representation of the modeling errors is derived via the calculation of a number of transfer functions from the input $\dot{q}_d$ to the output q. These transfer functions are included in the set of all possible transfer functions that arise from the maximum ±20% variations in the stability derivatives. For purposes of analysis, each of the three parameters, $\hat{M}_i$, $i = \alpha, q, \delta_s$, takes on only three values: $0.8M_i$, M_i, and $1.2M_i$. All possible combinations of the linear transfer functions, for the same nominal system, are calculated. To cover the operating envelope without thrust vectoring, the standard F/A-18 suffers wing rock at angles of attack greater than 45 deg and ceases to be a stable flight test platform. With the addition of thrust vectoring, the HARV is stable and maneuverable up to 70-deg angle of attack.[1] Linear models at four different angles of attack—5, 20, 35, and 50 deg—are used in the development of an error model.[27] Magnitude and phase plots for $\alpha = 5$ and 35 deg are shown in Fig. 3.

The resulting transfer function model describing the set of possible linear input-output relationships between $\dot{q}$ and $\dot{q}_d$ is defined by $(1.04 + 0.21\delta_2)/(s + 1.2\delta_1)$ with $-1 \le \delta_1$ and $\delta_2 \le 1$. The term δ_1 corresponds to pole variations and δ_2 corresponds to gain variations in the linearized transfer function models. This set of transfer functions can be represented by the following LFT in the control problem formulation:

$$\begin{bmatrix} \dot{q} \\ z_1 \\ z_2 \\ q \end{bmatrix} = \begin{bmatrix} 0 & 1 & 1 & 1.04 \\ 1.2 & 0 & 0 & 0 \\ 0 & 0 & 0 & 0.21 \\ 1 & 0 & 0 & 0 \end{bmatrix} \begin{bmatrix} q \\ w_1 \\ w_2 \\ \dot{q}_d \end{bmatrix} \tag{11}$$

Each z_i is connected to w_i through δ_i for $i = 1, 2$.

V. Initial Outer-Loop Controller Synthesis

Two outer-loop controllers (based on different performance objectives) using μ techniques are synthesized and analyzed. The first, denoted as K_q^1, is based on feeding back the pitch rate measurement only, whereas the second controller, denoted as K_q^2, makes use of both pitch rate measurement as well as the integral of pitch rate. The pitch rate and angle measurements are assumed to be corrupted by sensor noise.

It is desirable to avoid actuator saturation. This can be accomplished by weighting the deflection and deflection rate of the actuators; however, using the dynamic inversion formulation, the actuator dynamics are not directly accessible. Thus a weight on the output of the μ controller, the desired pitch acceleration, is used to limit the control bandwidth. For purposes of synthesis, the maximum deflections are ±10.5 deg (0.183 rad) and ±16 deg (0.279 rad) for the stabilizers and TVC, respectively. For this flight condition $M_{\delta_s} = -0.735\ 1/s^2$ and $M_{\delta_{TVC}} = -1.683\ 1/s^2$. These conditions limit the maximum pitch acceleration to

$$|\dot{q}|_{\max} = 0.735 * 0.183 + 1.683 * 0.279 = 0.604 \left[\frac{\text{rad}}{s^2} \right] \tag{12}$$

Using this value, the pitch acceleration weight is

$$W_q = \frac{1}{0.604} \frac{1 + (s/bw)}{1 + (s/100)} \left[\frac{1}{s^2} \right] \tag{13}$$

where bw is a bandwidth parameter to be selected.

The pitch rate, handling quality transfer function between the stick command and the pitch rate was derived from the idealized short period aircraft response.[29,30] This transfer function is

$$\frac{q_{hq}}{\text{stick}} = \frac{K_q[1 - (s/Z_w)]}{(s^2/\omega_{sp}^2) + (2\zeta_{sp}/\omega_{sp})s + 1} \tag{14}$$

Recent research on handling qualities at high angles of attack indicated that pilots prefer to have lower short period frequency and higher damping factors as trim angle of attack increases. Using data from Ref. 29, the short period damping factor and natural frequencies were selected as $\zeta_{sp} = 1$ and $\omega_{sp} = 1$ rad/s. The numerator zero, Z_w, was selected to be -0.312, the open-loop value at an angle of attack of 20 deg. The gain K_q was selected to be 0.115 rad/s/in. so that a maximum stick deflection of 2.5 in. would command the estimated maximum pitch rate. These handling quality parameters provide level 1 response from 0 to 30-deg angle of attack.[29,30] Data on handling qualities for higher angles of attack are not yet accessible in the open literature. The desired handling quality parameters could have been scheduled with angle of attack, but this would have involved some scheduling of the outer-loop controller.

The weighting function W_q on the error between the actual pitch rate and the pitch rate generated by the handling quality model is

$$W_q = 57.3 \frac{1 + (s/100)}{1 + (s/3)} \left[\frac{1}{\text{rad/s}} \right] \tag{15}$$

The preceding handling quality model and weighting function on the pitch rate errors lead to a bandwidth of 4 rad/s. Thus a value of $bw = 4$ rad/s was used in the pitch acceleration weight given in Eq. (13) to limit controller bandwidth.

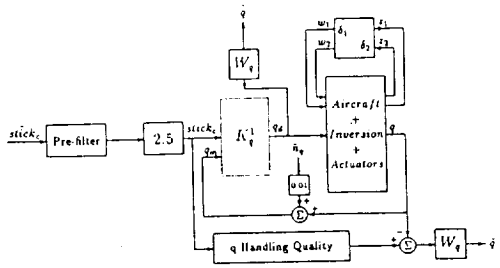

Fig. 4 K_q^1 configuration: interconnection structure for robust dynamic inversion synthesis in pitch rate.

In the original flight control system, the pilot stick command was prefiltered to avoid unwanted high-frequency stick inputs. This filter had the transfer function

$$\text{stick}_c = \frac{24.65}{s^2 + 6.28s + 9.86} \tag{16}$$

Since the filter was part of the original system, it was also included in the interconnection model along with the weighings and the definition for the inner-loop model uncertainty given in Eq. (11). The interconnection model including sensor noise for the first μ controller synthesis is shown in Fig. 4.

Relating this interconnection to the standard formulation given in Fig. 1 results in the following definitions for the inputs and outputs:

$$\begin{aligned} z &= [z_1 \quad z_2 \quad \tilde{q} \quad \tilde{\dot{q}}_d]' \\ w &= [w_1 \quad w_2 \quad \text{stick}_c \quad \tilde{n}_q]' \\ y &= [\text{stick}_c \quad q_m]' \\ u &= \dot{q}_d \end{aligned} \tag{17}$$

The resulting controller, denoted K_q^1, was 13th order. As described in the next section, this controller yielded good transcient response, but its steady-state response was not satisfactory. A second μ controller K_q^2, which incorporated the integral of the pitch rate, was designed and improved the steady-state response.

VI. Controller Evaluation and Outer-Loop Redesign

The performance of the controllers are evaluated using a detailed nonlinear simulation of the HARV.[30] This simulation includes the six degree-of-freedom nonlinear dynamics, high-order models of actuator and sensor dynamics, limits on control surface deflections and rates, and aerodynamic coefficients obtained from look-up tables as functions of angle of attack and Mach number. The baseline lateral-directional controller used is provided within the simulation. The flap settings are determined by a Mach number and angle-of-attack schedule. There are no elastic modes of the aircraft included in the simulation.

The pitch rate responses with controller K_q^1 implemented are shown in Fig. 5a for a doublet stick input. Figure 5a illustrates the pitch rate calculated from the nonlinear simulations at two different trim angles of attack, $\alpha = 5$ and 35 deg, and the output of the linear handling quality model. Note that all of the short-term pitch rate responses are very close to one another; however, as time increases, the angle of attack of the aircraft drifts from its steady-state value as shown in Fig. 5b. This is because the steady-state pitch rate is not zero. The drift is more pronounced at higher initial angles of attack and is due to implementation of a controller that was designed using the short period mode only.

Two linear plant descriptions are used to analyze controller K_q^1. The first model was only a short period approximation of the aircraft. The second model included the phugoid and the short period modes of the aircraft. The estimated parameters used in the dynamic inversion are varied according to the relationships given in Eq. (11). When analyzing the four-state model, only the two short period states were fed back for the inversion. The linear models for the analyses were at 5, 20, 35, and 50 deg. For each angle of attack, 27

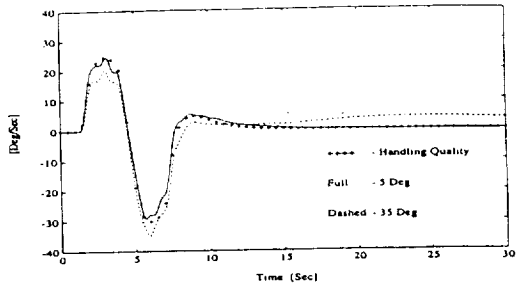

a) Pitch rates of the 2 nonlinear simulations and handling quality

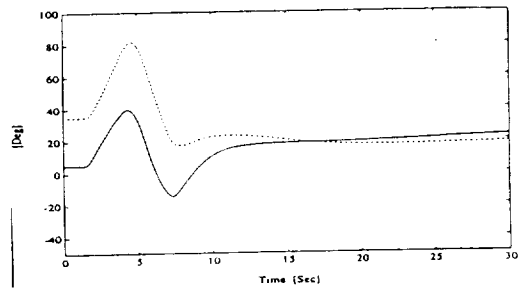

b) Angles-of-attack

Fig. 5 Nonlinear simulations starting at α = 5 and 35 deg with μ controller K_q^1.

cases were analyzed. This resulted in 108 cases for the short period approximation and 108 simulations for the four-state longitudinal model. The results of this analysis are as follows:

1) All of the closed-loop models were stable using the short period approximation.

2) With the four-state model, unstable closed-loop modes were found. The smallest time constant of instability was about 20 s.

3) For the short period approximation, α is stabilized by the stabilization of q.

It is well known that integral control improves robustness to parameter uncertainties and helps to eliminate steady-state tracking errors. The simulation results presented earlier indicated very good short-term tracking. The long-term performance was not as impressive as the short period response, due to the divergence of α. This divergence was the result of a nonzero, long-term pitch rate. As it will be seen, the addition of an integrator leads to a very robust system with respect to both performance and stability. The new control problem formulation, which includes the integral of pitch rate, is shown in Fig. 6.

A pitch rate integration is added to the controller. To enforce zero pitch rate error at steady state in the H_∞ framework, a θ handling quality model must be included. This is accomplished by integrating the output of the pitch rate handling quality model and weighting the difference between the output of this integrator and θ by W_θ. Synthesizing an H_∞ controller for the formulation shown in Fig. 6 leads to an extremely large H_∞ norm due to the addition of the integrator on the θ handling quality model. This problem is solvable, using the state-space solution, if the subsystem relating the disturbances w, to the measurements y does not lose rank on the imaginary axis.[21] This means that the subsystem from w to y should be observable and controllable on the imaginary axis. Adding an integrator to the handling quality model, without bringing its output to the controller, leads to the integrator state being neither observable nor controllable at the origin. To overcome this problem, the integrator is approximated as $1/(s + 0.0001)$. The weighting function on the error in θ is defined as

$$W_\theta = 28.65 \frac{1 + (s/25)}{1 + (s/0.5)} \left[\frac{1}{\text{rad}}\right] \tag{18}$$

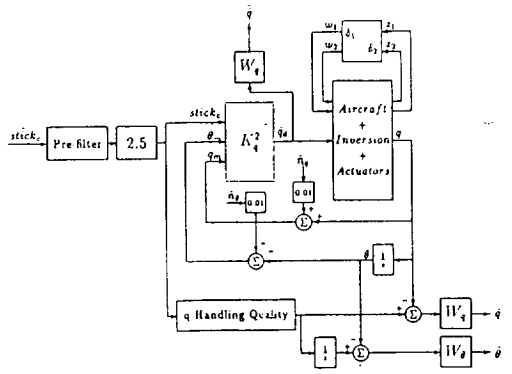

Fig. 6 K_q^1 configuration: interconnection structure for robust dynamic inversion synthesis in pitch rate.

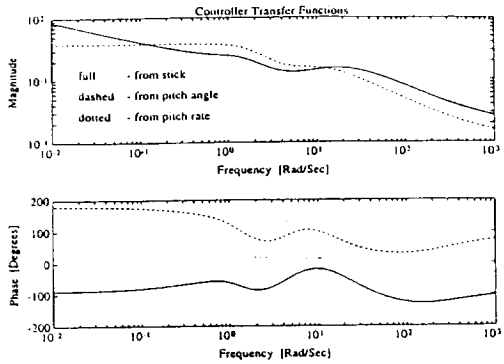

Fig. 7 Bode plots of μ controller K_q^2.

The noise added to θ measurement is assumed to be white with zero mean and spectral density of 0.01 rad/$\sqrt{\text{rad/s}}$.

The μ synthesis was applied to the modified formulation. Only a single $D-K$ iteration step was required to achieve the lowest possible μ. The controller K_q^2 consisted of 16 states. Its transfer functions are shown in Fig. 7. The integral nature of the stick to $\dot{q}_d$ transfer function is apparent. The robust performance μ that was achieved is 1.149 with the robust stability μ being 0.311. The μ plots are shown in Fig. 8. The low value of the robust stability μ implies very good robustness characteristics. This is shown to be true from the nonlinear as well as from the linear analyses that were performed on the closed-loop system with controller K_q^2. Since the robust performance μ value was not less than 1, we are only guaranteed to achieve 87% of the performance objectives for 87% of the size of the uncertainty.

The same simulations presented in Fig. 5 are performed again with controller K_q^2 implemented. Figure 9 shows the time histories of the most important longitudinal variables. As in Fig. 5, Fig. 9a shows two nonlinear pitch rate responses together with the linear handling quality model pitch rate response for the given stick input. The nonlinear responses compare extremely well with the linear response. Comparing Fig. 9a with Fig. 5a shows that the differences in the amplitudes between the pitch rates is smaller for the K_q^2 controller than for the K_q^1 controller. The difference is very significant in the long-term behavior of the system. Steady-state errors on the pitch rates are eliminated, and the long-term angle-of-attack responses do not diverge. The stabilizer did not saturate in deflection; however, the deflection and rate of the TVC vanes saturated for very short time periods in some cases.

The controller based on nonlinear inversion with the μ controller, which includes the integral of pitch rate, provides very good

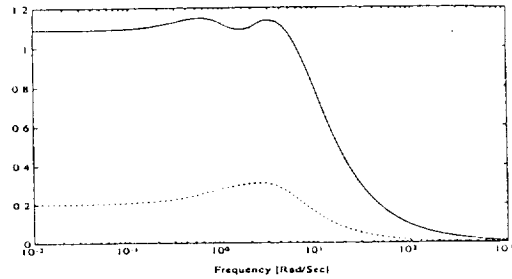

Fig. 8 Upper bounds for robust performance and robust stability μ for controller K_q^2.

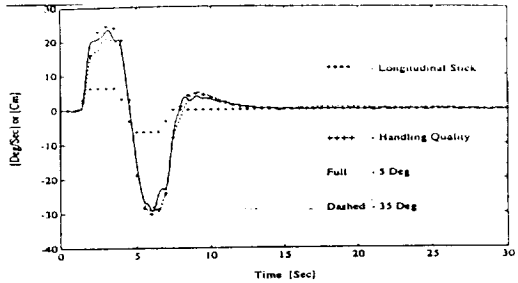

a) Pitch rates of the 2 nonlinear simulations, handling quality and stick Input

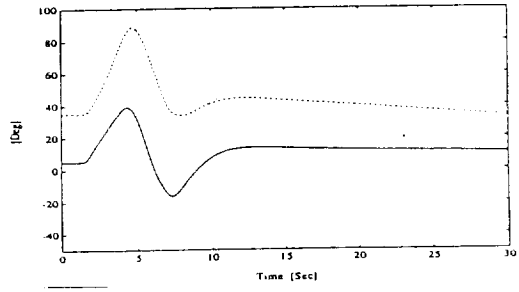

b) Angles-of-attack

Fig. 9 Nonlinear simulations starting at α = 5 and 35 deg with μ controller K_q^2.

nominal performance. The following tests were applied to evaluate the robustness of the controller:

1) Addition of a constant to the feedback linearization scaling: this test was accomplished by scaling the linearizing feedback by +20% or −20%.

2) Addition of white noise to the linearizing feedback scaling: instead of being 1, the new scaling is $(1+\sigma)$ where σ is white noise with zero mean and standard deviation of 0.2

3) Six degree-of-freedom maneuvers: a longitudinal stick input is applied simultaneously with lateral stick commands that excite lateral dynamics.

All of the tests were performed with noisy measurements.

The second test is the most severe and is illustrated in Figs. 10 and 11. This test uses a very high frequency time-varying scaling error in the linearizing feedback. The white noise model on the scaling has unlimited bandwidth. Note the high-frequency noise on the actuator rates shown in Fig. 11. This is due to the direct feed through to the actuators of the linearizing feedback. This actuator

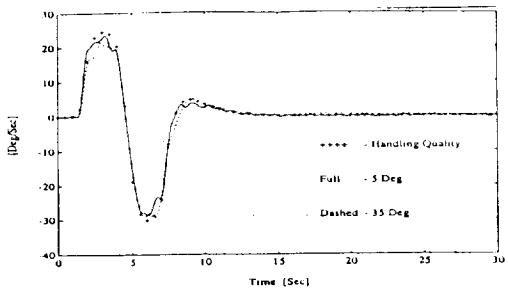

a) Pitch rates of the 2 nonlinear simulations handling quality

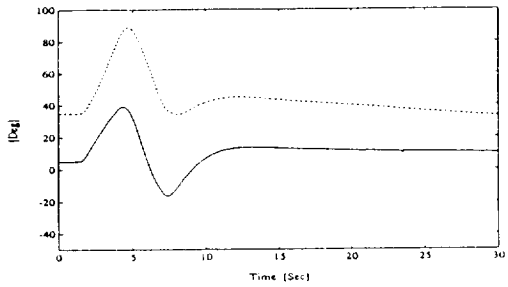

b) Angles-of-attack

Fig. 10 Nonlinear simulations starting at α = 5 and 35 deg with the relation Torque$_c$ = Torque$_c$(1 + noise).

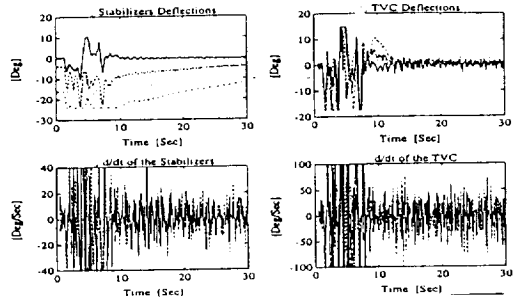

Fig. 11 Nonlinear simulations starting at α = 5, 20, 35 and 50 deg with the relation Torque$_c$ = Torque$_c$(1 + noise).

noise has almost no effect on the pitch rate response as seen in Fig. 10.

The third nonlinear test, not shown in the paper, examined the ability to decouple the pitch rate response from nonlinear in roll and yaw dynamics.[24] A lateral stick doublet of ±2.0 in. was followed by a longitudinal stick doublet of the same amplitude. The lateral stick was applied to excite the lateral dynamics. It was observed that even at the roll and yaw rates of up to 100 and 25 deg/s, respectively, good decoupling was achieved. In all of the decoupling tests the pitch rates closely measured the response of the handling quality model and almost no longitudinal response was observed when applying only the lateral stick.[27] Hence, it can be concluded that the decoupling properties of the robust dynamic inversion controller are satisfactory.

A linear analysis was performed for controller K_q^2 similar to the one described for controller K_q^1. As with controller K_q^1, the short period approximations of the aircraft exhibited no right-half plane poles. For the full longitudinal approximations, only three unstable poles resulted. The fastest unstable time constant was 400 s compared with 20 s for controller K_q^1. This is a significant improvement.

VII. Conclusions

The robust dynamic inversion methodology described in this paper has applicability to a wide range of flight control design problems. It provides low-order, robust control laws that require little scheduling with flight conditions. The resulting dynamic response is excellent over a wide range of angles of attack and Mach numbers.

Acknowledgment

This research was supported by NASA Langley Research Center, Grant NAG 1-1380, with Bart Bacon as technical monitor.

References

[1]Dornheim, M. A., "X-31, F-16 MATV, F/A-18 HARV Explore Diverse Missions," *Aviation Week & Space Technology*, April 18, 1994, pp. 46–47.

[2]Chiang, R. Y., Safonov, K. P., and Tekawy, J. A., "A Fixed H_∞ Controller for a Supermaneuverable Fighter Performing the Herbst Maneuver," *Proceedings of the 29th Conference on Decision and Control* (Honolulu, HI), Dec. 1990, pp. 2599–2606.

[3]Voulgaris, P., and Valvani, L., "High Performance Linear-Quadratic and H_∞ Designs for a 'Supermaneuverable' Aircraft," *Journal of Guidance, Control, and Dynamics*, Vol. 4, No. 1, 1991, pp. 157–165.

[4]Ostroff, A. J., "High-Alpha Application of Variable Gain Output Feedback Control," *Journal of Guidance, Control, and Dynamics*, Vol. 15, No. 2, 1992, pp. 491–497.

[5]Sparks, A., and Siva, B., "Application of Structured Singular Value Synthesis to a Fighter Aircraft," *Journal of Guidance, Control, and Dynamics*, Vol. 16, No. 5, 1994, pp. 940–947.

[6]Falb, P. L., and Wolovich, W. A., "Decoupling in the Design and Synthesis of Multivariable Control Systems," *IEEE Transactions on Automatic Control*, Vol. AC-12, No. 6, 1967, pp. 651–659.

[7]Singh, S. N., and Rugh, W. J., "Decoupling in a Class of Nonlinear Systems by State Variable Feedback," *Journal of Dynamic Systems, Measurement, and Control*, Dec. 1972, pp. 323–329.

[8]Singh, S. N., and Schy, A. A., "Output Feedback Nonlinear Decoupled Control Synthesis and Observer Design For Maneuvering Aircraft," *International Journal of Control*, Vol. 31, No. 4, 1980, pp. 781–806.

[9]Meyer, G., and Cicolani, L., "Application of Nonlinear Systems Inverses to Automatic Flight Control Design—System Concept and Flight Evaluations," *Theory and Application of Optimal Control in Aerospace Systems*, AGARD, AG251, 1981, pp. 10.1–10.29.

[10]Meyer, G., Su, R., and Hunt, R., "Application of Nonlinear Transformations to Automatic Flight Control," *Automatica*, Vol. 20, No. 1, 1984, pp. 103–107.

[11]Menon, P. K., Badgett, M. E., and Walker, R. A.,"Nonlinear Flight Test Trajectory Controllers for Aircraft," *Proceedings of the AIAA Guidance and Control Conference* (Snow Mass, CO), AIAA, New York, 1985, (AIAA-85-1890-CP).

[12]Asseo, S. J., "Decoupling of a Class of Nonlinear Systems and Its Application to an Aircraft Control Problem," *Journal of Aircraft*, Vol. 10, No. 12, 1973, pp. 739–747.

[13]Lane, S. H., and Stengel, R. F., "Flight Control Design Using Nonlinear Inverse Dynamics," *Automatica*, Vol. 24, No. 4, 1988, pp. 471–483.

[14]Snell, S. A., Enns, D. F., and Garrard, W. L., "Nonlinear Inversion Flight Control for a Supermaneuver Aircraft," *Journal of Guidance, Control, and Dynamics*, Vol. 15, No. 4, 1992, pp. 976–984.

[15]Bugajski, D. J., and Enns, D. F., "Nonlinear Control Law with Application to High Angle-of-Attack Flight," *Journal of Guidance, Control, and Dynamics*, Vol. 15, No. 3, 1992, pp. 761–767.

[16]Buffington, J., Adams, R., and Banda, S., "Robust, Nonlinear, High-Angle-of-Attack Control for a Supermaneuverable Vehicle," *Proceedings of the AIAA Guidance, Navigation, and Control Conference* (Monterey, CA), AIAA, Washington, DC, 1993, pp. 690–700, (AIAA Paper 93-3774).

[17]Elgersma, M. R., "Control of Nonlinear Systems and Application to Aircraft," Doctoral Thesis, Univ. of Minnesota, Minneapolis, MN, 1988.

[18]Slotine, J. E., and Li, W., *Applied Nonlinear Control*, Prentice-Hall, Englewood Cliffs, NJ, 1991.

[19]Balas, G. J., Reiner, J., and Garrard, W. L., "Robust Dynamic Inversion Control Law for Aircraft Control," *Proceedings of the AIAA Guidance, Navigation, and Control Conference* (Hilton Head, SC), AIAA, Washington, DC, 1992, pp. 192–205.

[20]Balas, G. J., Reiner, J., and Garrard, W. L., "Design of a Flight Control System for a Highly Maneuverable Aircraft Using μ Synthesis," *Proceedings of the AIAA Guidance, Navigation, and Control Conference* (Monterey, CA), AIAA, Washington, DC, 1993.

[21]Balas, G. J., Doyle, J. C., Glover, K., Packard A. K., and Smith, R., "The μ Analysis and Synthesis Toolbox User's Guide," MUSYN, Inc., and The Mathworks, May 1991.

[22]Packard, A. K., Doyle, J. C., and Balas, G. J., "Linear, Multivariable Robust Control with a μ Perspective," *ASME Journal of Dynamics, Measurements and Control: Special Edition on Control*, Vol. 115, No. 2b, 1993, pp. 426–438.

[23]Doyle, J. C., "Analysis of Feedback Systems with Structured Uncertainties," *Proceedings of the IEE-D*, Vol. 129, 1982, pp. 242–250.

[24]Doyle, J. C., Lenz, K., and Packard, A. K., "Design Examples Using μ Synthesis: Space Shuttle Lateral Axis FCS During Reentry," *IEEE CDC*, Dec. 1986, pp. 2218–2223.

[25]Doyle, J. C., "Lecture Notes on Advances in Multivariable Control," *ONR/Honeywell Workshop on Advances in Multivariable Control*, Minneapolis, MN, Oct. 1984.

[26]Doyle, J. C., Glover, K., Khargonekar, P., and Francis, B. A., "State Space Solutions to Standard H_2 and H_∞ Control Problems," *IEEE Transactions on Automatic Control* Vol. AC-34, No. 8, 1989, pp. 831–847.

[27]Reiner, J., "Control Design for Aircraft Using Robust Dynamic Inversion Technique," Ph.D. Thesis, Univ. of Minnesota, Minneapolis, MN, July 1993.

[28]Sontag, E. D., *Mathematical Control Theory, Deterministic Finite Dimensional Systems*, Springer-Verlag, New York, 1990.

[29]Anon, "Flying Qualities of Piloted Aircraft," MIL-STD-1797A," March 1987.

[30]Krekeler, G., Wilson, D. J., and Riley, D. R., "High Angle-of-Attack Flying Qualities Criteria," AIAA 28th Aerospace Sciences Meeting, AIAA Paper 90-0219, Reno, NV, Jan. 1990.

[31]Bettrill, C. S., Arbuckle, P. D., and Hoffler, K, "Simulation Model of a Twin-Tail High Performance Airplane," NASA Langley Research Center Report, Hampton, VA, 1990.